AIP Journal of Applied Physics

Temperature- and electric-field-dependent polarization rotations in (211)-cut Pb (Mg 1/3 Nb 2/3) 0.69 Ti 0.31 O 3 (PMNT31%) single crystal

Chi-Shun Tu, L.-W. Hung, R. R. Chien, and V. Hugo Schmidt

Citation: Journal of Applied Physics **96**, 4411 (2004); doi: 10.1063/1.1789270
View online: http://dx.doi.org/10.1063/1.1789270
View Table of Contents: http://scitation.aip.org/content/aip/journal/jap/96/8?ver=pdfcov
Published by the AIP Publishing

Temperature- and electric-field-dependent polarization rotations in (211)-cut $Pb(Mg_{1/3}Nb_{2/3})_{0.69}Ti_{0.31}O_3$ (PMNT31%) single crystal

Chi-Shun Tu[a] and L.-W. Hung
Department of Physics, Fu Jen University, Taipei 242, Taiwan, Republic of China

R. R. Chien and V. Hugo Schmidt
Department of Physics, Montana State University, Bozeman, Montana 59717

(Received 23 February 2004; accepted 11 July 2004)

Polarization rotations of temperature- and electric-field-dependent phase transformations in a (211)-cut $Pb(Mg_{1/3}Nb_{2/3})_{0.69}Ti_{0.31}O_3$ (PMNT31%) single crystal were observed by means of polarizing microscopy. Dielectric permittivity was also measured as a function of temperature and frequency. Below 380 K domains are mostly rhombohedral (R) phase mixed with monoclinic (M) domains. As temperature increases above 380 K, polarizations of the rhombohedral domains begin to rotate toward the cubic (C) phase through monoclinic distortions, i.e., $R \rightarrow M \rightarrow C$, associated with a long-range percolation of monoclinic phase near 380 K. However, the tetragonal phase was not observed apparently. Electric-field-dependent domain structures show that a long-range $R \rightarrow M$ phase transformation takes place in the range of 3–5 kV/cm as electric field increases. The crystal cannot reach a monodomain as the electric field reaches 26 kV/cm. A hysteresis loop of polarization versus electric field was also measured for comparison with electric-field-dependent observation of polarizing microscopy. © *2004 American Institute of Physics*.
[DOI: 10.1063/1.1789270]

I. INTRODUCTION

Relaxor-based ferroelectrics $Pb(Mg_{1/3}Nb_{2/3})_{1-x}Ti_xO_3$ (PMNT), which have a morphotropic phase boundary (MPB) between rhombohedral (R) and tetragonal (T) phases for $0.26 \leqslant x \leqslant 0.36$,[1] have attracted attention because of their high performance on piezoelectric related applications. Monoclinic (M) and orthorhombic (O) have also been reported in PMNT system.[2–8] It has been found that most physical properties of PMNT system strongly depend on Ti concentration, strength of external electric (E) field, crystallographic orientation, history, and even sample scale (powder, ceramic, or single crystal).[2–13] Compositional heterogeneities (or spatial phase segregation) are commonly observed in these materials. Furthermore, the ultrahigh piezoelectric response has been theoretically attributed to polarization rotations through intermediate M or O phases.[14] In poled $Pb(Zr_{1-x}Ti_x)O_3$ ceramic, an M phase was reported over a narrow composition near MPB, playing a key role in connecting the $\langle 001\rangle T$ and $\langle 111\rangle R$ phases.[15]

By a neutron x-ray diffraction, an M_C-type M phase was evidenced for unpoled PMNT ceramics with $31 \leqslant x \leqslant 37$ in the low-temperature region, in which M phase was mixed with R, T, or O phases.[2] M_B-type and M_C-type M phases were also found in unpoled PMNTx ceramics for $27\% \leqslant x \leqslant 30\%$ and $31\% \leqslant x \leqslant 34\%$, respectively.[6] By means of polarizing microscopy, a sequence of temperature-dependent phase transformations $R \rightarrow M \rightarrow C$ was proposed in a (111)-cut PMNT33% single crystal.[3] Coexistence of R and M phases has been found in a (001)-cut PMNT33% single crystal at room temperature by means of polarizing microscopy analysis.[16] The M phase seems to be intrinsic in the PMNT system for compositions near the MPB.

An external dc bias can induce phase transformations, which depend strongly on orientation and amplitude of E field. From synchrotron x-ray diffraction, an M_A-type M phase was observed in a (001)-cut PMNT35% crystal with a prior poling ($E = 43$ kV/cm), but unpoled and weakly poled PMNT35% samples exhibit an average R symmetry.[4] A sequence of field-induced phase transitions $R \rightarrow M_A \rightarrow T \rightarrow M_A \rightarrow R_{111}$ was proposed by means of a polarizing microscope on a (111)-cut PMNT33% with an E field applied along [111].[5] From our recent study of field-induced polarization rotation on a (001)-cut PMNT24% crystal, it was found that polarizations of R domains rotate toward the [001] tetragonal T_{001} phase through M_A-type M distortions, i.e., $R \rightarrow M_A \rightarrow T_{001}$, as E field increases along [001].[17] But it cannot reach a T_{001} monodomain even when the field reaches 44 kV/cm.[17] On the other hand, a $R \rightarrow O \rightarrow T$ phase transition was suggested from the dielectric results on a (011)-cut PMNT33% crystal with a prior poling E field (<4 kV/cm) along [011], but for $E > 5$ kV/cm a $R \rightarrow O$ transition was proposed at room temperature.[7] A field-induced $R \rightarrow O$ transformation through an M_B-type M distortion was proposed on a (110)-cut PMNT30% crystal.[8] Note that transformations of $R \leftrightarrow O, O \leftrightarrow T$, or $R \leftrightarrow T$ are of first order.

It is believed that polarization rotation through intermediate phases (M or O) plays a key role in high piezoelectric performance in PMNT materials. The correlation between polarization rotation and physical parameters, such as crystallographic orientation and strength of external E field, is a practical issue to discover. In this report, temperature- and E-field-dependent domain structures were investigated on a

[a]Author to whom all correspondence should be addressed; electronic mail: phys1008@mails.fju.edu.tw

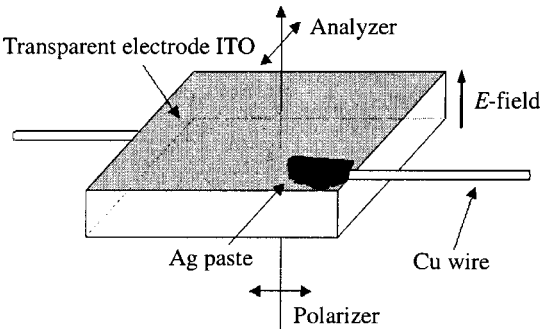

FIG. 1. Experimental configuration for domain observation.

(211)-cut PMNT31% single crystal, because the (211)-cut would be the most sensitive for observing movement of *M* phase domains.

II. EXPERIMENTAL PROCEDURE

The lead magnesium niobate–lead titanate crystal PMNT31% was grown using a modified Bridgman method. The sample was cut perpendicular to the ⟨211⟩ direction. Gold electrodes and transparent conductive films of indium tin oxide (ITO) were deposited, respectively, on sample surfaces by radio frequency sputtering for dielectric measurement and *E*-field-dependent domain observation. Before any measurement described below, the sample was annealed above T_m which corresponds to the dielectric maximum. For domain observation, a Nikon E600POL polarizing microscope was used with a 0°/90° crossed polarizer/analyzer (P/A) pair. The experimental configuration is given in Fig. 1. The sample thickness is about 55 μm. For *E*-field-dependent domain observation, a dc field was applied along [211]. All domain patterns were observed under a perpendicularly crossed P/A pair.

For dielectric measurements, a variable-frequency Wayne-Kerr Precision Analyzer PMA3260A with four-lead connections was used to obtain capacitance and resistance. A Janis CCS-450 closed cycle refrigerator was used with a Lakeshore Model 340 temperature controller. The temperature ramping rate was 1.5 K/min. The dielectric data were taken upon cooling from the cubic phase first, and then heating without a dc *E* field or a prior poling. The hysteresis loop of polarization versus *E* field (PEF) was measured at room temperature by using a Sawyer-Tower circuit at frequency 46 Hz.

III. REVIEW OF OPTICAL EXTINCTION AND POLARIZATION

The propagation direction $\vec{k}$ of the polychromatic "white" light is along [211] for this work. Most of the information is obtained from observation of optical extinction, which occurs if the following conditions are satisfied: (1) there must be no optical activity for the direction $\vec{k}$, (2) either $\vec{k}$ must lie along an optical axis or $\vec{k}$ is not along an optical axis, the incident $\vec{E}$ must lie along one of the two perpendicular axes in the plane perpendicular to $\vec{k}$ for which the optical-frequency permittivity is maximum or minimum. A more detailed review was presented in Refs. 3 and 18.

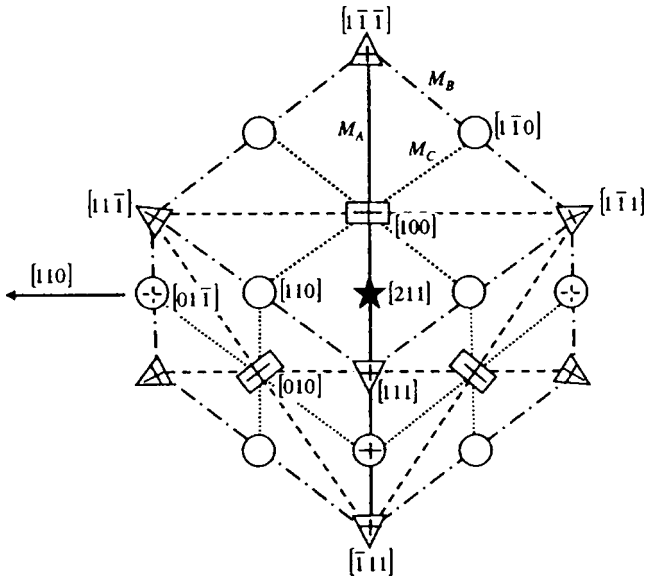

FIG. 2. Relations among various phases and corresponding polarizations viewed along [211].

Figure 2 shows the (211)-cut projection of relations among the various phases and corresponding polarizations for the primitive unit cell ($Z=1$) and double-size orthorhombic cell ($Z=2$). Rectangles indicate the directions of tetragonal polarization vectors **P**. Triangles indicate directions for rhombohedral **P**'s. Circles indicate directions for orthorhombic **P**'s. Solid, dash-dot, and dashed lines indicate directions that polarizations can take for monoclinic cells based on the double-size ($Z=2$) orthorhombic cell. Dotted lines alternate between rectangles and circles, indicating directions that polarizations can take for monoclinic cells based on the simple ($Z=1$) cubic cell. Any polarization whose direction does not correspond to one of the three symbol types or four types of lines results from a triclinic cell. Figure 3 gives angles between polarization projections viewed along [211] for various *R*, *T*, and *O* domains shown in Fig. 2. Domains that are optically inactive for $\vec{k}$ along [211] will have extinction for

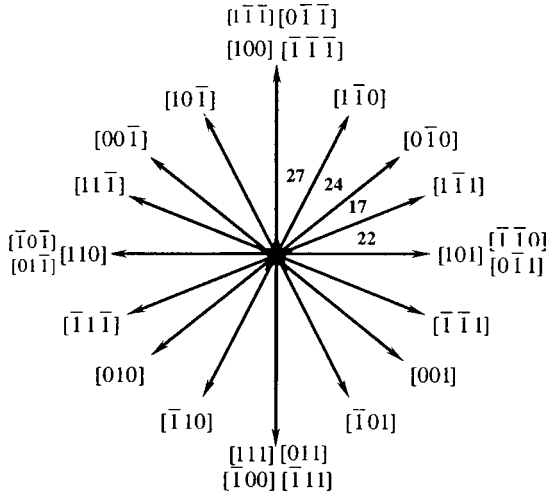

FIG. 3. Angles between various *R*, *T*, and *O* domains projected along [211].

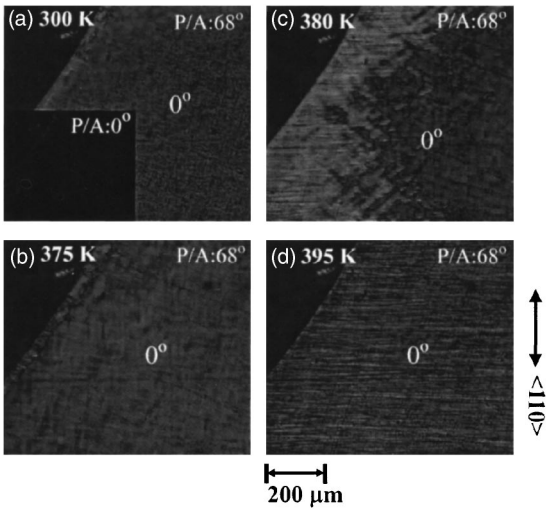

FIG. 4. Temperature-dependent domain structures observed at P/A:68° upon heating.

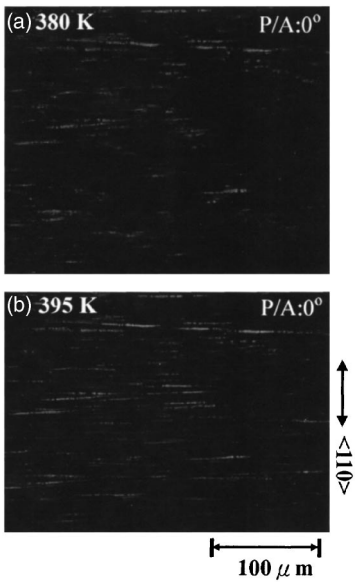

FIG. 5. Domain structures at 380 and 395 K observed at P/A:0°.

optical electric field along the radial and circumferential axes indicated by solid crossed lines inside the symbols in Fig. 2. *O* domains that are optically active will not have extinction for optical electric field along the radial and circumferential axes indicated by dashed crossed lines inside the symbols. *O* domains that have incomplete extinction due to some reasons (except optical activity) are given by open circles. Solid lines between some symbols indicate no shift in extinction directions away from those in symbols connected by these lines. Lines for the remaining $Z=2$ (dashed and dash-dot) and all $Z=1$ (dotted) *M* polarization directions indicate shift in extinction direction away from radial and circumferential. The central "black" star indicates the M_A polarization (**P**) direction parallel to $\hat{k}$. A concise and clear mathematical analysis for the general extinction problem appears in Sommerfeld.[19] A detailed treatment was published by Hartshorne and Stuart.[20]

The M_C cell **P** lies between two adjacent *T* and *O* **P** vectors. The M_A cell has **P** between two adjacent *T* and *R* **P** vectors, whereas the M_B cell has **P** between two adjacent *R* and *O* **P** vectors. The M_B "phases" in our opinion should be called a single phase, whose cell is based on the $Z=2$ orthorhombic cell. Most higher-symmetry phases (*O*,*R*, or *T*) with nearby polarization **P** directions are related directly by monoclinic or triclinic phases. For instance, as shown in Fig. 2, rotation of polarization **P** from the *R*-domain $[\bar{1}11]$ direction to the *T*-domain [100] direction can proceed via a monoclinic M_A cell with highest-symmetry principal axis b_m along $[01\bar{1}]$.

IV. RESULTS AND DISCUSSION

A. Temperature-dependent phase transformations

Figure 4 shows temperature-dependent domain structures. "P/A:68°" at the upper-right corner indicates that the domain picture was taken when the angle between one of the P/A pair axes and the [110] direction is 68°. Hereafter, the P/A angle is with respect to the [110] direction. The "0°" indicates that the domain matrix exhibits optical extinction at 0° with respect to [110], i.e., one of the P/A pair axes is parallel to [110]. The black area at the upper-left corner in each picture of Fig. 4 is the background. As shown in the inset of Fig. 4(a), at 300 K the whole domain matrix exhibits extinction along the [110] direction, i.e., P/A:0°. When observing the (211)-cut sample along [211] between a perpendicularly crossed P/A pair, as shown in Fig. 2, *R*,*T*, and *O* phases have extinction angle at 0°. In addition, M_A-type *M* domains may show extinction at 0° as indicated by the solid line in Fig. 2. From a synchrotron x-ray diffraction, coexistence of *R* and M_C-type *M* phases was found in PMNT31% ceramic at 20 and 300 K.[2] The M_C-type *M* distortion which connects *T* and *O* phases does not exhibit extinction at 0°. In this study, there is no apparent evidence of *T* phase at 300 K. If *T* domains exist in the sample, extinction would be more likely also seen at 39° (see Fig. 3), which was not found. Besides, the 90° domain wall that *T* phase usually is associated with was not observed either. On the other hand, the (211) cut is not suitable to determine the existence of *O* domain due to incomplete extinction (except optical activity). An *O* phase was so far only proposed in (011)-cut PMNT30% (Ref. 8) and PMNT33 (Ref. 7) single crystals with an *E* field applied along [110]. Thus, at 300 K domains are most likely *R* phase mixed with *M* domains.

As shown in Fig. 4(b), the extinction of domain matrix keeps at 0° up to about 375 K. The stripelike domains begin to appear significantly near 380 K as shown in Fig. 4(c). These stripelike domains distribute in the domain matrix which exhibits extinction at 0°. To identify extinction angles of the stripelike domains, the domain structures are enlarged in Fig. 5 for 380 and 395 K, respectively. These domains have various nonzero extinction angles, such as $\sim 22°$, $\sim 30°$, and $\sim 62°$ at 380 K and $\sim 24°$, $\sim 32°$, and $\sim 50°$ at 390 K. As temperature increases above 380 K, the stripelike domains expand gradually over the domain matrix. As shown in Fig. 6, the real part ε' of dielectric permittivities exhibits a steplike anomaly near 385 K upon heating. This long-range transformation was also manifested by a peak (whose posi-

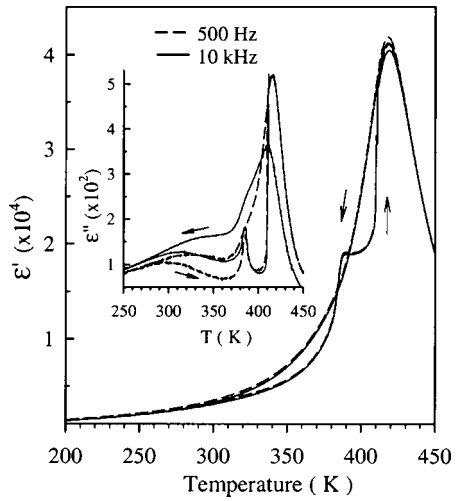

FIG. 6. Temperature-dependent dielectric permittivity ε' obtained at 500 Hz and 10 kHz upon heating and cooling processes. The inset is the imaginary part ε'' of dielectric permittivity.

tion is independent of frequency, but not the amplitude) and a shoulder near 385 K in the imaginary part ε'' upon heating and cooling, respectively, as illustrated in the inset of Fig. 6. The discrepancy in dielectric anomalies between cooling and heating runs implies that thermal activated polarization rotations are different during cooling and heating processes. A total extinction which corresponds to the cubic phase, begins to appear near 415 K and soon occupies the entire crystal near 420 K. It is consistent with $T_m \sim 420$ K which corresponds to the dielectric maximum of real part ε'.

What is the phase between 380 and 420 K? When observing the (211)-cut sample along [211] between a crossed P/A pair, the allowed extinction angles for *T* domains are 0°, 39°, or 51° measured from the ⟨110⟩ axis. Similarly, the allowed extinction angles for *R* domains are 0° or 22°. Thus, in the region of 380–420 K most of the domains are *M* phase. In other words, near 380 K polarizations of the *R* mixed with *M* domains are activated by thermal energy and begin to rotate through *M* distortions. A long-range transformation from *R* macrodomains to *M* macrodomains most likely takes place near 380 K, perhaps mixed with *T* domains in a small fraction before the crystals go into the cubic.

B. Electric-field-induced phase transformations

The *E*-field-dependent domain structures, as shown in Fig. 7, were taken at room temperature with P/A:45°. The angles shown in different regions of Fig. 7 are extinction angles with respect to the [110] direction. At $E=0$ kV/cm [Fig. 7(a)], the domain matrix exhibits an extinction angle at 0°, indicating a *R* phase mostly. "*C*" indicates a crack caused by the polishing process. "*N*" indicates the area without ITO thin film. With increasing *E* field as shown in Fig. 7(b), the domain matrix exhibits apparent change in the range of 3–5 kV/cm, which is consistent with the coercive field $E_C \sim 4$ kV/cm of the PEF hysteresis loop measured at room temperature as given in Fig. 8.

As *E* field increases, the domain matrix exhibits various nonzero extinction angles, such as ~10°, ~46°, and ~72°

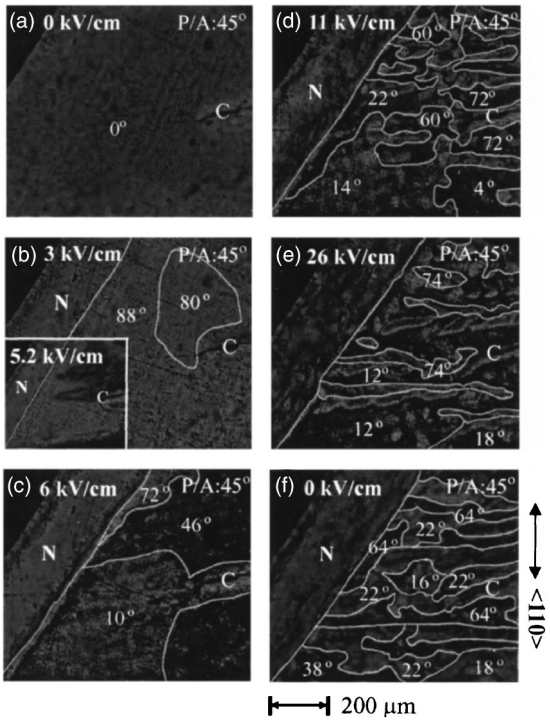

FIG. 7. Electric-field-dependent domain structures observed at room temperature.

at $E=6$ kV/cm [Fig. 7(c)]; ~4°, ~14°, ~22°, ~60°, and ~72° at $E=11$ kV/cm [Fig. 7]. As given in Fig. 3, the possible extinction angles for *R* and *T* domains are 0° or 22° and 0° or 39°, respectively. Thus, most of the *R* domains already transformed into *M* domains via polarization rotations before *E* field reached 6 kV/cm. In other words, a long-range $R \rightarrow M$ phase transformation takes place in the range of 3–5 kV/cm. A similar field-induced $R \rightarrow M_A$ transformation was observed on a (001)-cut PMNT24% crystal with *E* field applied along [001].[17] Note that the *O* domain cannot be identified from this (211)-cut sample. Furthermore, at $E=26$ kV/cm the domain matrix exhibits extinctions at various angles, such as ~12°, ~18°, and ~74°, all of which correspond to monoclinic phase. It indicates that a [211] *M* monodomain cannot be achieved easily at room temperature.

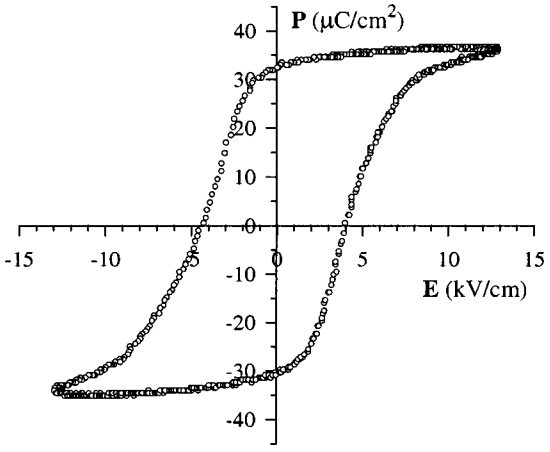

FIG. 8. Hysteresis loop of polarization vs *E* field obtained at room temperature.

The (001)-cut PMNT24% cannot reach a tetragonal monodomain either, even though the applied E field reaches 44 kV/cm.[17] However, R monodomain was easily induced near $E=12$ kV/cm on a (111)-cut PMNT33% crystal as E field was applied along [111].[3] With decreasing E field the crystal exhibits very different domains as shown in Fig. 7(f), in which most of domains persist in the M phase.

V. CONCLUSIONS

In this paper, it was evidenced that below 380 K domains are mostly R phase mixed with M domains in the (211)-cut PMNT31% crystal. As temperature increases above 380 K, polarizations of the R domains begin to rotate toward the cubic phase through M distortions. In other words, a long-range percolation of M phase takes place near 380 K. Most of the domains persist in the M phase and do not transform into the T phase before the crystal reaches the cubic phase near 420 K, i.e., $R \rightarrow M \rightarrow C$. One notes that the PMNT31% crystal should undergo a sequence of phase transformations $R \rightarrow T \rightarrow C$ according to the MPB for PMNT system.[1] However, the T phase was not observed apparently in the (211)-cut PMNT31% crystal. In fact, the PMNT31% crystal seems to prefer M distortions while crossing over from R to C phases. The polarization path, such as M_A, M_B, and M_C, of M distortions cannot be determined from this (211)-cut sample. We have also found the coexistence of R and M phases in another piece of (211)-cut PMNT31% single crystal, in which the M phase also persists until the cubic phase takes place.

With increasing E field at room temperature, a long-range $R \rightarrow M$ phase transformation takes place in the range of 3–5 kV/cm. Even at $E=26$ kV/cm the crystal cannot entirely reach an M monodomain. It seems that the M phase can be initiated by a small external field and activated by thermal energy as temperature increases.

ACKNOWLEDGMENTS

This work was supported by NSC Grant No. 92-2112-M-030-007 and DoD EPSCoR Grant No. N00014-02-1-0657.

[1] T. R. Shrout, Z. P. Chang, N. Kim, and S. Markgraf, Ferroelectr., Lett. Sect. **12**, 63 (1990).
[2] B. Noheda, D. E. Cox, G. Shirane, J. Gao, and Z.-G. Ye, Phys. Rev. B **66**, 054104 (2002).
[3] C.-S. Tu, V. H. Schmidt, I.-C. Shih, and R. Chien, Phys. Rev. B **67**, 020102 (R) (2003).
[4] Z.-G. Ye, B. Noheda, M. Dong, D. Cox, and G. Shirane, Phys. Rev. B **64**, 184114 (2001).
[5] C.-S. Tu, I.-C. Shih, V. H. Schmidt, and R. Chien, Appl. Phys. Lett. **83**, 1833 (2003).
[6] A. K. Singh and D. Pandey, Phys. Rev. B **67**, 064102 (2003).
[7] Y. Lu, D.-Y. Jeong, Z.-Y. Cheng, Q. M. Zhang, H. Luo, Z.-W. Yin, and D. Viehland, Appl. Phys. Lett. **78**, 3109 (2001).
[8] D. Viehland and J. F. Li, J. Appl. Phys. **92**, 7690 (2002).
[9] J. Han and W. Cao, Phys. Rev. B **68**, 134102 (2003).
[10] X. Zhao, B. Fang, H. Cao, Y. Guo, and H. Luo, Mater. Sci. Eng., B **96**, 254 (2002).
[11] Z. Li, Z. Xu, Z. Xi, X. Wei, and X. Yao, Opt. Mater. (Amsterdam, Neth.) **23**, 429 (2003).
[12] C. S. Tu, C. L. Tsai, V. H. Schmidt, H. Luo, and Z. Yin, J. Appl. Phys. **89**, 7908 (2001).
[13] C.-S. Tu, C.-L. Tsai, J.-S. Chen, and V. H. Schmidt, Phys. Rev. B **65**, 104113 (2002).
[14] H. Fu and R. E. Cohen, Nature (London) **403**, 281 (2000).
[15] R. Guo, L. E. Cross, S.-E. Park, B. Noheda, D. E. Cox, and G. Shirane, Phys. Rev. Lett. **84**, 5423 (2000).
[16] G. Xu, H. Luo, H. Xu, and Z. Yin, Phys. Rev. B **64**, 020102 (R) (2001).
[17] R. Chien, V. H. Schmidt, C.-S. Tu, L.-W. Hung, and H. Luo, Phys. Rev. B **69**, 172101 (2004).
[18] V. H. Schmidt, R. Chien, I.-C. Shih, and C.-S. Tu, AIP Conf. Proc. **677**, 160 (2003).
[19] A. Sommerfeld, *Optics* (Academic, New York, 1964), pp. 129–139.
[20] N. H. Hartshorne and A. Stuart, *Crystals and the Polarizing Microscope* (E. Arnold Ltd., London, 1970).